STATE RESEARCH CENTER OF RUSSIA
INSTITUTE FOR HIGH ENERGY PHYSICS

IHEP 2002-37

V.V. Babintsev*, V.A. Bumazhnov, Ju.V. Gilitsky, A.G. Denisov

RPC PROTOTYPE SIMULATION FOR TOF MEASUREMENT

* e-mail: *babintsev@mx.ihep.su*

Protvino 2002

UDK 539.12.142 M–24

Abstract

Babintsev V.V., Bumazhnov V.A., Gilitsky Ju.V., Denisov A.G. RPC prototype simulation for TOF measurement.: IHEP Preprint 2002-37. – Protvino, 2002. – p. 16, figs. 12, tables 3, refs.: 23.

RPC multigap gas detector can be used as a TOF detector at PHENIX. The simulation results of a RPC prototype detector are presented. It is shown that one can achive good intrinsic time of flight resolution (up to 50 ps). It is proposed to dispose such type of the detector at the front face of EMCAL.

Аннотация

Бабинцев В.В., Бумажнов В.А., Гилицкий Ю.В., Денисов А.Г. Моделирование высокоомной плоскопараллельной газовой камеры (RPC) : Препринт ИФВЭ 2002-37. – Протвино, 2002. – 16 с., 12 рис., 3 табл., библиогр.: 23.

Представлены результаты моделирования RPC прототипа, который может быть использован в качестве TOF детектора на установке PHENIX. Показано, что временное разрешение может достигать величины 50 пс. Использование такого относительно простого и компактного детектора в комбинации с калориметром может дать хорошее временное, координатное и энергетическое разрешение.

Introduction

Last years the good results have been obtained with RPC gas detectors (Resistive Plate Chambers) in the field of the TOF resolution. Using the multigap RPCs one can improve the time resolution by reducing the gap size and increase the low efficiency of a single thin gap by using several gaps integrated in the same detector and read out by the same system of pads [1].

The multigap RPC is usually made of 4-6 gas-gaps of 200-300 μm each. It was shown that time-of-flight resolution of 4-gaps RPC can be better than 50 ps with the detection efficiency up to 99% for MIPs [2].

Good time resolution obtained for some RPCs prototypes was also demonstrated in the article [21]. It was found that in the range of 0.3-0.6 mm gap width, the time resolution is a linear function of the gap width with the slope of 13 psec/100 μm for the gas type based on the freon mixture. They have shown that for the gap width of 0.3 mm and counting rate less than 500 Hz/cm^2 one can achive the time resolution about 70 ps.

The same time resolution was demonstrated in the multigap RPC with the gas-mixture 90% $C_2H_2F_4$ 5% *isobutane* and 5% SF_6 which is close to our choise: 95% $C_2H_2F_4$ 5% *isobutane*. The induced signal is a sum from a large number of small gas gaps (d=0.22 mm). It is a prototype of TOF array for the ALICE experiment [16]. They used resistive glass plate marked as "Schott A2 (A14)" with the measured resistivity in the range $(1.5 - 8) * 10^{12}$ Ω cm. The measured time jitter of the amplifier and discriminator was to be 50 ps. The prototype efficiency was greater than 99% for high energy particles. The value of the applied electric field was about 10 kV/mm.

Such RPC detector can be used as a TOF detector at PHENIX.

To check the parameters dependence of the RPC prototypes it is desirable to simulate such type of the detectors. One of the simulation methods has been suggested by M.Abbrescia [3]. The model of the simulation of the avalanche grouth and pulse development is based on the Townsend theory of avalanches taking place in an RPC.

RPC detector description

With the aim to have large detection efficiency of the MIP-signals (greater than 95%) a RPC prototype is proposed as a multi-gap detector. In Fig. 1 one can see the schema of 5-gaps RPC prototype.

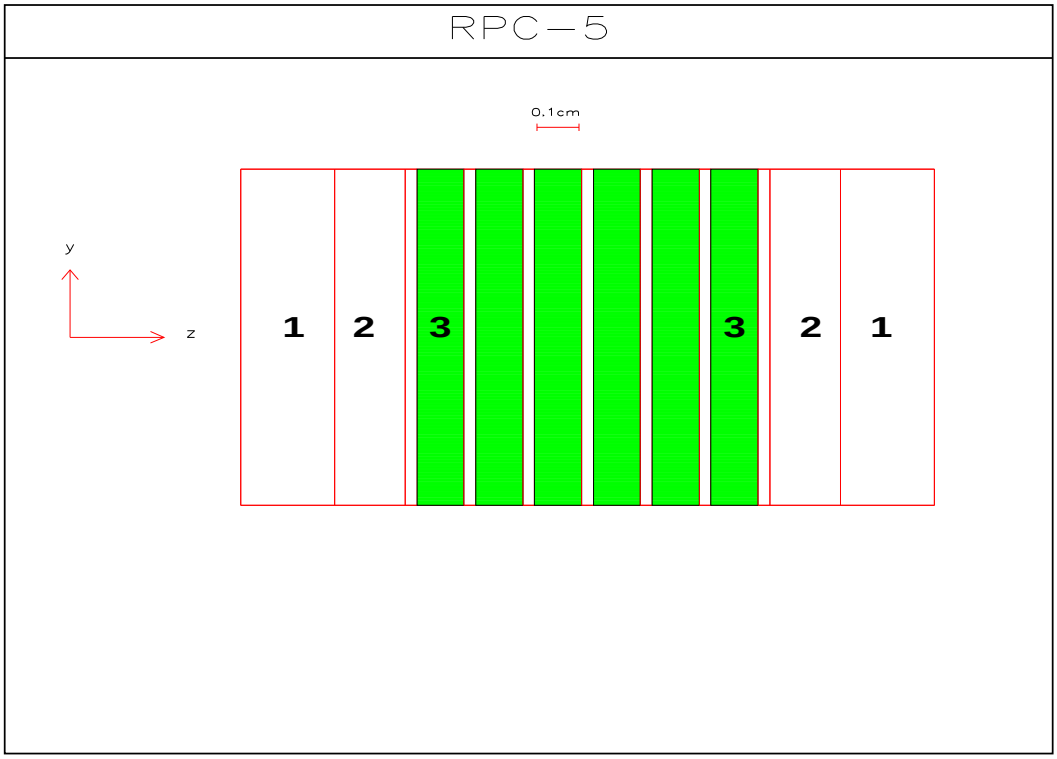

Figure 1. 5-gaps RPC prototype (crossection). Shaded boxes (3) are glass plates. (1) are the cells for collection of an induced signal. (2) is an isolator. Between (2) and (3) the conductor board is situated for high voltage supply.

Pick-up electrodes (signal cells) are depicted schematically. It is supposed that signal cell has dimensions of 1 * 3 * 67 cm^3 fitting the Super Model of EMCAL PHENIX. The cross-section of the signal cell is the box of $1 * 3$ cm^2 dimension where the walls have 2 mm width.

Signals generated by gaseous avalanches are induced on the external electrodes and collected on the both sides of the RPC detector to measure "X" and "Y" coordinates of the incident charge particles.

An isolator (2) of the 1.5 mm width is situated between pick-up electrode (1) and high voltage supply electrode. Shaded boxes are the glass plates of the 1 mm width. The gas-gap has 0.2-0.3 mm width. The total width of the RPC prototype is about 2.5 cm. The avalanche development has a duration about 1-3 nsec. In glass RPSs, the recovery time is long enough ($\approx$ 1 sec), because of high resistivity ($\rho = 5 * 10^{12}$ Ω cm) and high dielectric permittivity ($\epsilon = 7$) [11] of float glass.

The charge spot from the avalanche on a glass plate is included in an disk with diameter less than 2 mm. The charge deposed on the electrodes is gradually absorbed into the surrounding plate. The time taken for this to happen, and hence for the electric field in the immediate area of the discharge to return to its applied value, is the recovery time for the RPC. This time can be expressed as

$$\tau = RC = \rho * \epsilon * \epsilon_0.$$

For $\epsilon = 7$ and for the float glass $\rho = 10^{12}$ it gives about 1 sec.

The RPC detector can be disposed on the front face of EMCAL (at the distance of 5 m from the primary vertex). Taking into account the measured intensity of secondary particles detected by EMCAL at PHENIX for different beams one can suppose that the flow intensity of secondary particles will not be higher than 30 Hz per cell (strip). This intensity cannot influence the detection efficiency and the process of restoring local voltage value after discharge in a gap after an avalanche creation.

The gas properties

The gas mixture composition affects RPC operation. Different gases are characterized by different values of primary ionization density λ. Generally it is between 2 and 8 (1/mm).

The cluster size distribution is known experimentally for a few gas (Ar, iC_4H_{10}, He, CO_2), for others one have to rely on the theoretical predictions. For some gases one can find experimentally measured electron multiplicity distributions in a cluster [12].

The present choice to operate RPCs with freon-based gas mixtures (instead of old magic $Ar/iso - C_4H_{10}$ mixture) basically is due to the low streamer probability together with high efficiency [4]. Further gases are needed as quenchers to prevent the chamber going into continues discharge : spare photoelectrons from the radiative decay of excited gas atoms and spare electrons escaping from the main avalanche can both lead to the development of secondary avalanches. Complex polyatomic molecules such as isobutane have many rotational and vibrational excited states, and hence can be used to absorb photons emitted by the deexcitation process in order to inhibit streamer formation. They absorb photons over a wide energy range, and then dissipate the energy through radiationless interactions and dissociation. A highly electronegative gas, such as freon, is needed to clear up peritheral electrons around the main body of the avalanche and so reduce the lateral spread of the discharge. This helps to minimize the area of electrode occupied by an avalanche unless the number of recombination photons is large.

Gases (and freon in itself) added to the gas-mixtures to absorb UV (ultra violet) photons created in an avalanche are methane (CH_4), ethane (C_2H_6), butane (C_4H_{10}), isobutane (C_4H_{10}) e.t. [13]. The influence of the UV photons in the creation of afterpulses is shown in the article [18]. When the gas in use cannot absorbe the total flux of UV photons there is high probability of others discharges which have long duration up to 1.7 μs. The time-period of such pulses can be defind as

$$T_g = T_- + (\tau_1 - \tau_L),$$

where T_- is the time of electron-flight in a gap; τ_1 — the mean life time of the exited molecules, $\tau_L = 1/(\eta V_d)$. This is a broad distribution with the center at T_g [19].

The avalanche process is a complex one where there is a lateral development associated with the multiplication of charges. This is due to diffusion of electrons, the electrostatic repulsion of charges, the propagation of ionizing photons...

The comparision of the different gas mixtures is given in the article [7]. The addition of SF_6 to the gas mixtures normally used seems to have reduced drastically the streamer probability [15], but a broad peak at high values of induced charge appears. This behaviour might be due to the space charge effect in big avalanches [5]. The model of exponential growth of the avalanches does not accounts for the observed shape of the charge spectra at high operating voltages. Therefore it has been supposed that the avalanche development proceeds exponentially until the charge contained in the gap reaches a certain value (about 0.5 – 2 pC).

Gas parameters can be obtained with the help of the gas simulation program MAGBOLTZ [9] and the electric field simulation program GARFIELD [10]. GARFIELD is a computer program for the detailed simulation of two- and three-dimensional drift chambers which includes drifting of particles, diffusion, avalanching and current induction. MAGBOLTZ computes transport properties for electrons in various gases, including drift velocity, the longitudinal and transverse diffusion coefficients and the Townsend and attachment coefficients.

Calculated gas parameters for our choise (Freon 134a or tetrafluoroethane $C_2H_2F_4(95\%)$ and isobutane (iC_4H_{10})) are presented in Fig. 2.

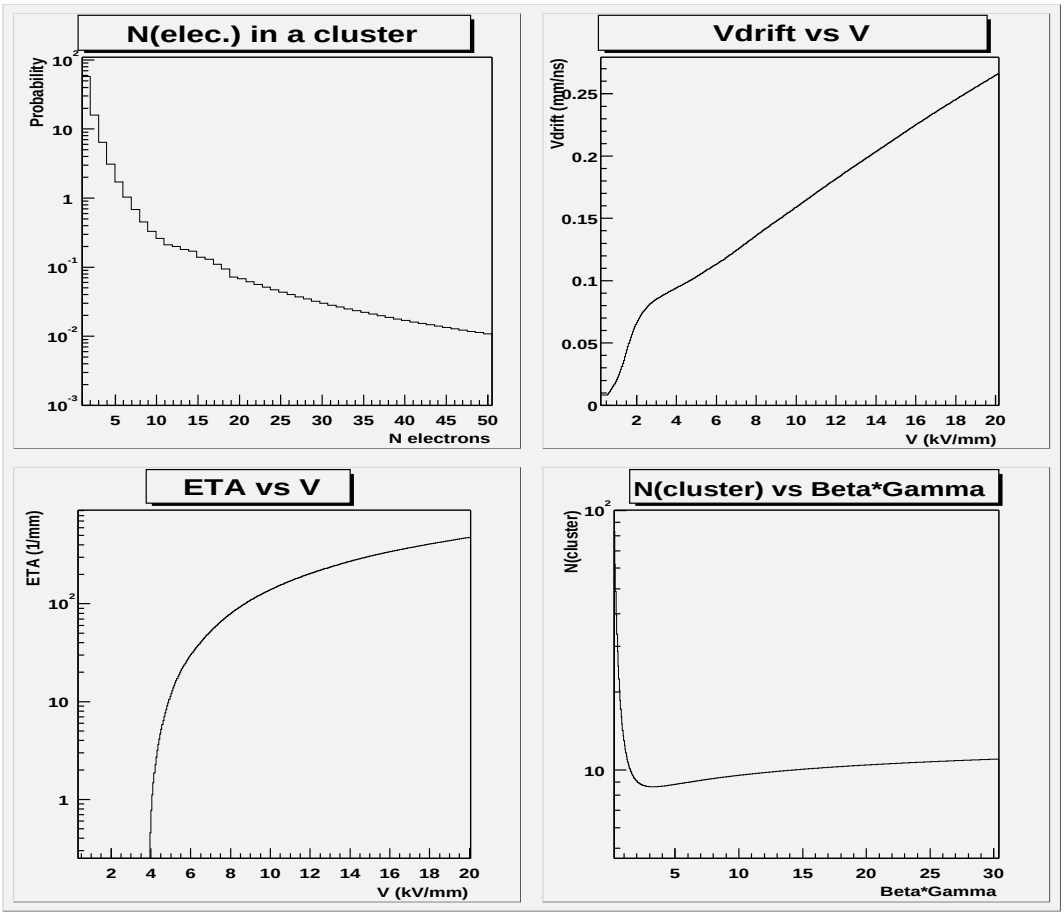

Figure 2. Gas properties used for the prototype: distribution of electron multiplicity in a cluster; η and electron speed (v_d) dependence on the electric field; $\beta * \gamma$ dependence of the cluster density per mm.

The last picture in Fig. 2 depicts the dependence of the created cluster density along a particle track per 1 mm versus the particle energy (in units of $\beta * \gamma$). This dependence corresponds to the ionization energy loss function of charge particle in a medium. The energy dependence of number of electrons in a cluster is very weak compared to the energy dependence of cluster density, therefore it is supposed that the electron number distribution in a cluster does not depend on the electric field.

Comparison of our gas choise with the other ones is presented in the article [17].

The saturation effect

Photographs of avalanches show that they tend to be wedge-shaped with a rounded head – somewhat like elongated droplets. The length is dictated by the electron drift velocity in the field, and the radius by the electron diffusion:

$$r^2 = 4 * D * t.$$

The most likely model of an avalanche to streamer transition can be summed up as follows [14]. As the avalanche progresses the space-charge fields of the cloud of electrons and positive ions becomes important. When the number of electrons in the advancing head of the avalanche approches 10^6 the avalanche begins to slow down due to the attraction of the positive ions. When the number reaches 10^8 the space-charge field in the avalanche middle is practically cancelled out. The neighboring field around the avalanche is modified as though by a dipole (an example of electric field calculation of an avalanche one can find in [20]).

Some experiments detected the effect of a high efficiency RPC operation with small gas-gap and the restricted collected charge value [16] [2]. The authors explain these effects as a) there is some secondary electron emission from the cathode surface of the resistive plates and b) there is a mechanizm that strongly inhibits avalanche growth when the avalanche gets large (space-charge effect).

To take into account the space-charge effect or the saturation effect in the simulation one is letting an avalanche grow exponentially until the charge contained in it reaches a given value Q_{sat}. Then, in a crude approximation, the avalanche stops its development, and just drift towards the anode [6]. Q_{sat} value can be as big as 2 pC, corresponding to $1.2 * 10^7$ electrons, close to the Raether limit for avalanche streamer transition.

The auther suggests to consider the case of simulation when avalanche fluctuation is absent at all (M=1, see the model description below). All models accounting for avalanche fluctuations refer to a regime of small avalanches. At the limit to streamer transition, these models could be no more applicable. As a matter of fact, charge spectra obtained with M=1 condition are the closest to the experimental data.

Fonte [8] suggests the method of taking into account the charge effect. The effective Townsent coefficient depends now on the avalanche charge according to the expression

$$\eta(q) = \eta_0 \frac{Q_{sat}}{q + Q_{sat}}.$$

According to the data the value of Q_{sat} depends on the electric potencial, gas mixture and gas-gap value. Therefore this value can be chosen from experimental data for the given detector.

The experimental data show that charge spectra depends also on the quantum characteristics of the cathode (photons created by an avalanche can create additional clusters near the cathode due to emitted electrons from the cathode surface). That is why one should introduce in the simulation the probability parameter of additional cluster creation near cathode surface where the parameter value depends on the applied electric field. Therefore this parameter also can be adjusted from experimental data.

One of the processes which can create additional electrons in a gas medium is the process when the moving charge particle in medium is accompanied by some secondary particles ($\delta-$electrons, photons,..). According to the GEANT3.21 and GENAT4 simulation of the RPC-prototype it was observed that angle distributions of co-moving particles are uniform in the range of 0-90

degree relative to the particle direction. The probability to observe co-moving electrons in a gas-gap with the energy greater than 100 KeV around the primary particles (pions) with the energy 0.4-1.0 GeV is about 25% (the energy of secondary electrons has the range of 0.1-20 MeV) for 5-gap prototype. An example of generated $\delta-$electrons are presented in Fig. 3.

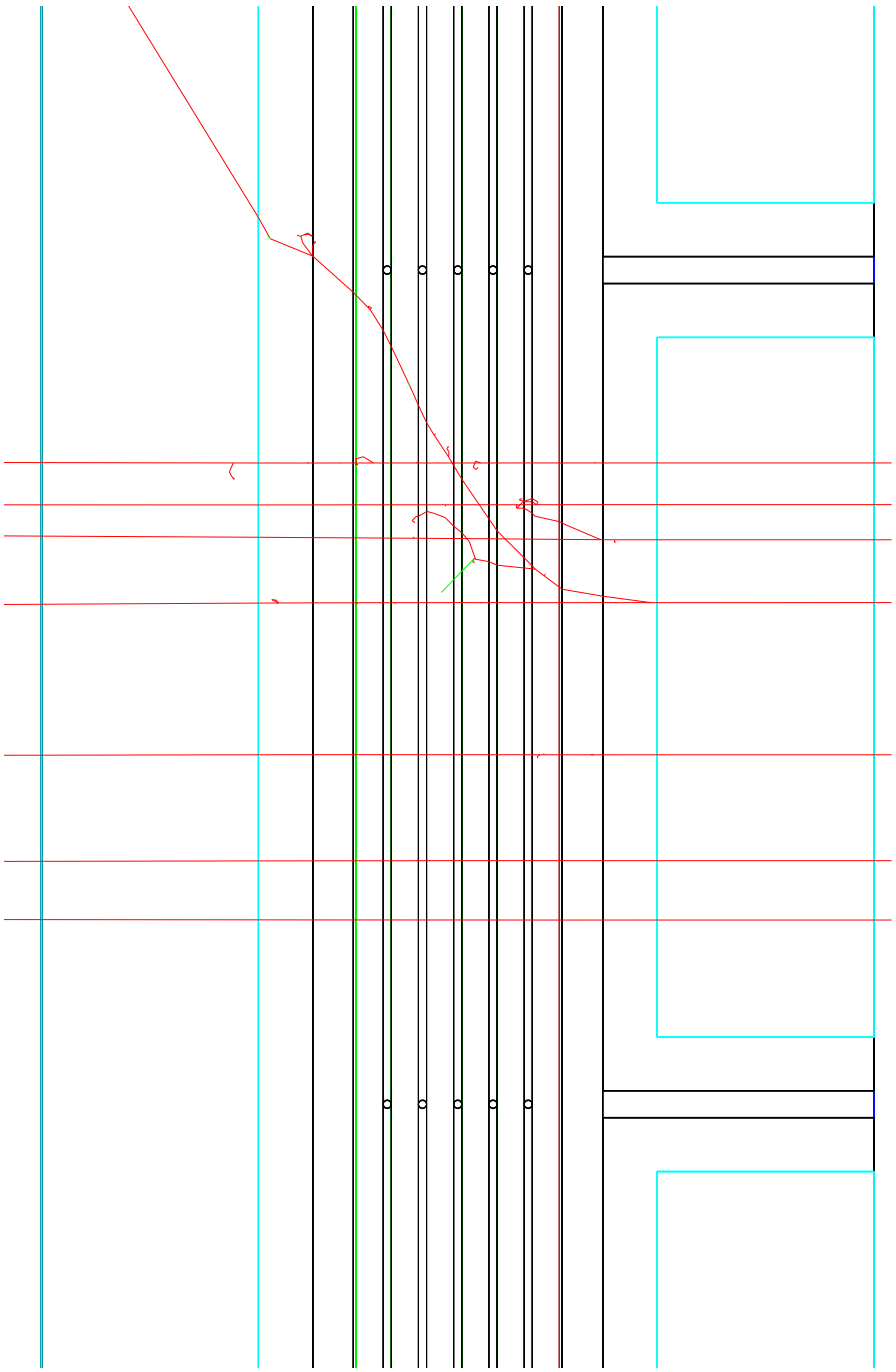

Figure 3. Example of generated $\delta-$electrons in the RPC prototype (enlarged crossection). Beam particles are moving from right to left.

The model description

The simulation program starts from generating n_{cl} primary ion-electron clusters created by an ionizing particle in a gas along its track [3]. The probability that "m" clusters are created in the gas-gap is given by the Poisson distribution

$$P_{cl}(n_{cl} = m) = \frac{(g\ \lambda_{eff})^m}{m} e^{(-g\ \lambda_{eff})},$$

where $\lambda_{eff} = \lambda/cos(\phi)$; λ is the number of primary ion-electron clusters created by the ionizing particle per unit length; ϕ is the angle of the incident particle (the angle between track of a particle and the perpendicular to RPC surface). "g" is the gas-gap width. The distributions of clusters inside the gap can be described by the product of probabilities to find (j-1) clusters before "x", j-th cluster at (x+dx) and (n-j) clusters after x at the distance of (g-x):

$$P^j(x + dx)dx = P^{j-1}(x)\ \lambda dx\ P^{n-j}(g - x).$$

Therefore x-dependence to find j-th cluster at the distance "x" in the gap can be expressed as (let us omit all coefficients)

$$f^j(x) = x^{j-1}\ (g - x)^{n-j}.$$

Taking into account the special cases for j=1 and j=n one can write:

$$f^j(x) = x^{j-1}\ (g - x)^{n-j}, \quad 1 <\ j\ < n;$$

$$f^j(x) = e^{-\lambda_{eff}\ x}, \quad n = 1;$$

$$f^j(x) = x^{j-1} * e^{-\lambda_{eff}\ x}, \quad j = n.$$

In Fig. 4 one can see an example of these distributions for the case of n=4 and gap=0.3 mm.

Assuming the exponential avalanche development, the total charge "q" at x-position is defined as

$$q(x) = \sum_{j=1}^{n_{cl}} q_e N_0^j M_j e^{\eta(x - x_0^j)},$$

where n_0^j is the number of primary electrons of the j-th cluster, η is the first effective Townsend coefficient. The factor M_j accounts for the stochastic fluctuations of the exponential grouth. For the high values of the electric field "E" (the case of the standart operation conditions for RPCs) the probability to find "n" electrons in an avalanche is given by a Polya distribution:

$$P(n_{av} = n) = [\frac{n}{N}(1 + \theta)]^\theta \exp[-\frac{n}{N}(1 + \theta)],$$

where for standart conditions $\theta = 0.5$ and $N = n_0 \exp[\eta(g - x_0)]$. M is a number randomly taken from this distribution devided by N. For a low and moderate electric field the probability that "n" electrons are produced after a path length $l = g - x_0$ is given by a Furry's law

$$P_F(n_{av} = n) = \frac{1}{N} e^{-n/N}, \quad N = n_0 e^{\eta(g - x_0)}.$$

Comparison of these two distributions is presented in Fig. 5.

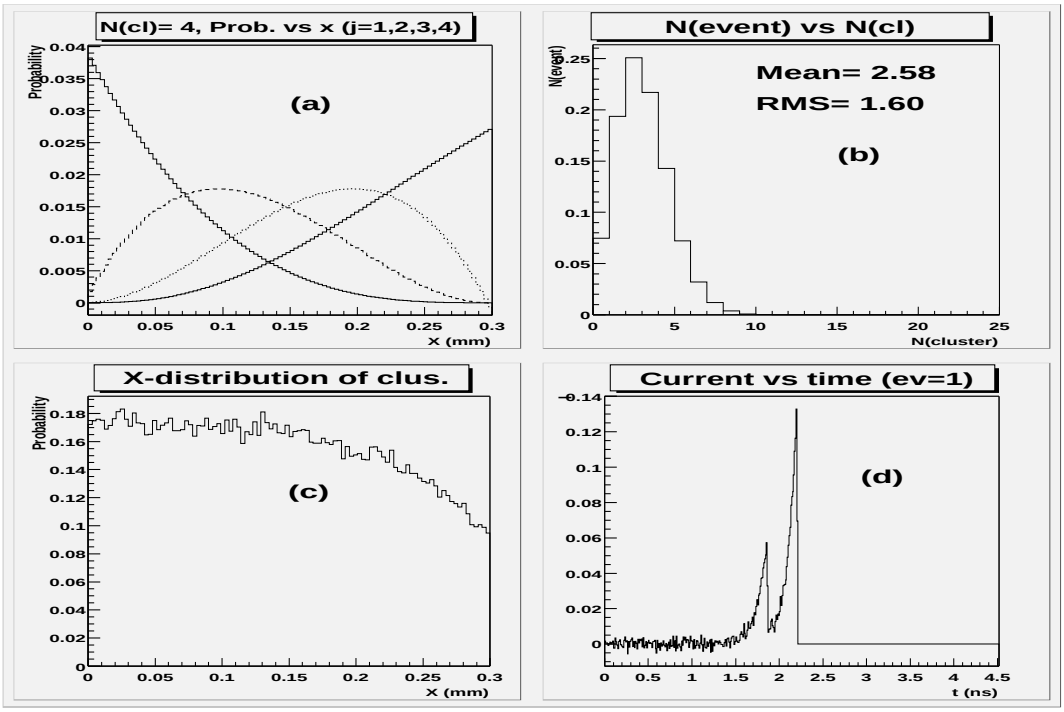

Figure 4. (a) Example of X-distribution of clusters (j=1,2,3,4) for n=4 created total number of clusters in a gap; (b) distribution of cluster number in a gap= 0.3 mm for MIP; (c) Total X-distribution of created clusters in a gap= 0.3 mm; (d) Current in Event=1 for 5-gap RPC detector.

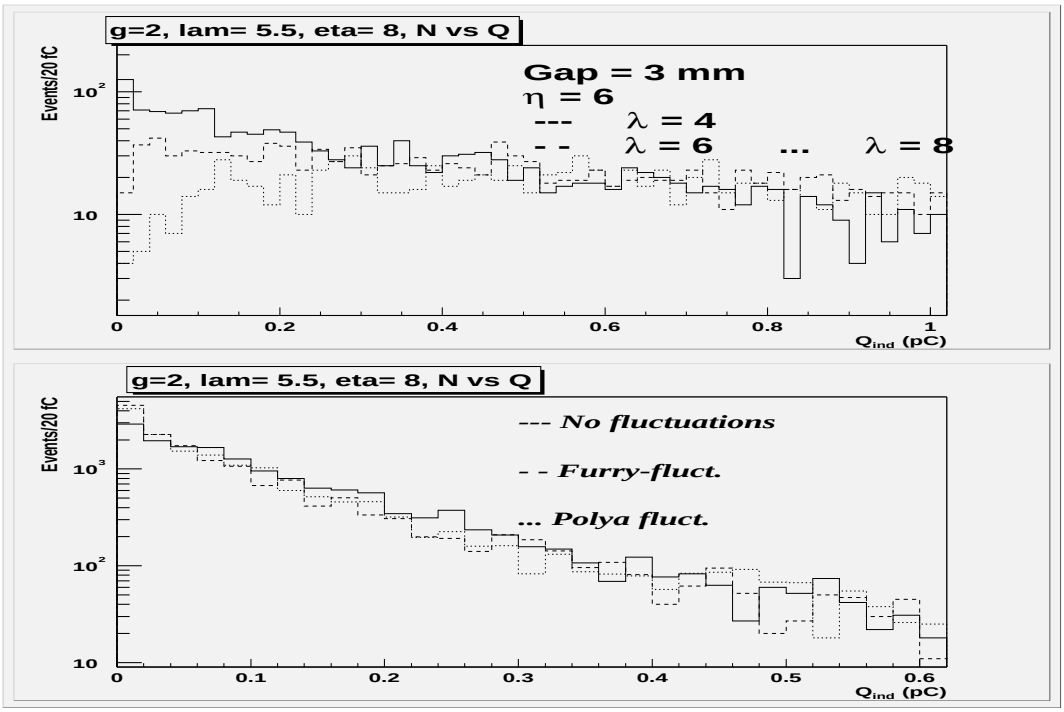

Figure 5. Top: N vs q_{ind} for different λ/η-ratios; Bottom: N vs q_{ind} with different fluctuation dependencies used.

Taking into account the glass electrode thickness "d" and its permittivity ϵ the weighting field E_w can be expressed through the drop of the weighting potencial in a gap [4]:

$$\Delta V_w = E_w\ g = \frac{\epsilon g}{n_g \epsilon g + (n_g + 1)d}.$$

"n_g" is the number of gaps in a detector. The current $I_{ind}(t)$ induced by a drifting charge on the external pick-up electrodes, as a function of time for one cluster is

$$I_{ind}(t) = -M\ q(t)\ v_d\ E_w.$$

"v_d" is the electron drift velocity and it is parallel to E_w. Or:

$$I_{ind}(t) = -v_d E_w q e^{\eta v_d \Delta t} \sum_{j=1}^{n_{cl}} n_0^j M_j.$$

The charge "q_{ind}" induced on pick-up electrodes is given by the expression

$$q_{ind} = \frac{q_e}{\eta g} \Delta V_w \sum_{j=1}^{n_{cl}} n_0^j M_j [e^{\eta(g - x_0^j)} - 1].$$

It was shown [3] that the distribution of the charge induced by the first cluster (the closest to the cathode) is given by

$$P_q(q_{ind} = q) = A q^{\frac{\lambda}{\eta} - 1},$$

where "A" is an appropriate renormalization constant. This behaviour is demonstarted in Fig. 5. It follows that to get good efficiency it is neccessary to use conditions where $\lambda/\eta > 1$.

It was observed that when the gain exceeds the value of $4.85 * 10^8$ the event is reffered to as a "streamer" one, when the collected charge does not depend on the initial ionization in a gas (the induced charge is one order of the value greater than the ordinary one).

The detector efficiency is defind by the fraction of events characterized by a charge greater than a certain electronic threshold q_{thr}.

Drifting electrons scatter on the gas molecules. Their motion can be described by their random motion, which is characterized by the mean energy "e" and gives rise to diffusion. The diffusion width of an electron cloud σ_x after starting point-like and traveled time interval "t" is

$$\sigma_x = \sqrt{2Dt} = \sqrt{\frac{2e_k x}{q_e E}},$$

where D — the diffusion coefficient, e_k- so called characteristic energy. The reality is more complex and one has two diffusion coefficient: longitudinal diffusion and transverse one ($D_L,\ D_T$). We do not take into account this random motion because of very high electron drift velocity in the high electric field.

Model summary

As it was stated above, for sufficiently high electric field (high gain region) there are two main processes which can give additional electron-cluster near the cathode: large amount of UV photons can reach the glass surface and $\delta-$electrons created by primary particle in glass (there is also a possibility of electron emission from the glass surface in a high electric field especially in the path-ionized region of the particle track). The appearance of additional electrons depends on the quantum characteristics of the used materials and the electric field value.

Another factor which define the measured charge distribution is connected with charge saturation effect observed for some gas mixtures (space-charge effect). This effect depends on the saturation parameter value (Q_{sat}) for each gas mixture (energy distribution of electrons, the ability to absorb UV photons,...).

In the RPC simulation program one can use the following possibilities to fit experimental distributions:

- general simulation (no saturation effect);
- the saturation effect is present, but $v_{drift} = const$;
- the saturation effect is present, v_{drift} is a variable parameter according to the η variation;
- the saturation effect is present, but $v_{drift} = const$ and the charge fluctuation in an avalanche is absent (M=1);
- the saturation effect is present, v_{drift} is a variable parameter according to the η variation and the charge fluctuation in an avalanche is absent (M=1).

In the program one can change v_{drift} according to the η variation using their dependence on the applied electric field. There is the possibility to change Polya-distribution parameter (default one equals 0.5) because of the saturation effect. As it was mentioned by Abbrescia [6] the fluctuation distributions are known only for small charge values of an avalanche. In the case of charge saturation one has to change the law of fluctuation and may be to eliminate it at all (M=1). For small values of Polya-distribution parameter the value of charge fluctuation in an avalanche is small enough also.

Therefore one can use the following parameters to fit experimental distributions

- Q_{sat} value parameter;
- the Polya-distribution parameter Pol or set M=1;
- the probability $Prob$ to obtain an additional electron cluster near the cathode in each gap.

In Fig. 6 one can see the induced charge distributions for one gap RPC detector for 3 different voltage values for 3 cases: a) general simulation (no parameters); b) Q_{sat}= 1 pC; c) Q_{sat}= 1 pC and $Prob$=0.6 (one can find additional electron cluster at X=0 with probability Prob=0.6). There was used the general Polya distribution for the charge fluctuation. It follows from Fig. 6 that charge distribution is very sensitive to the used parameters.

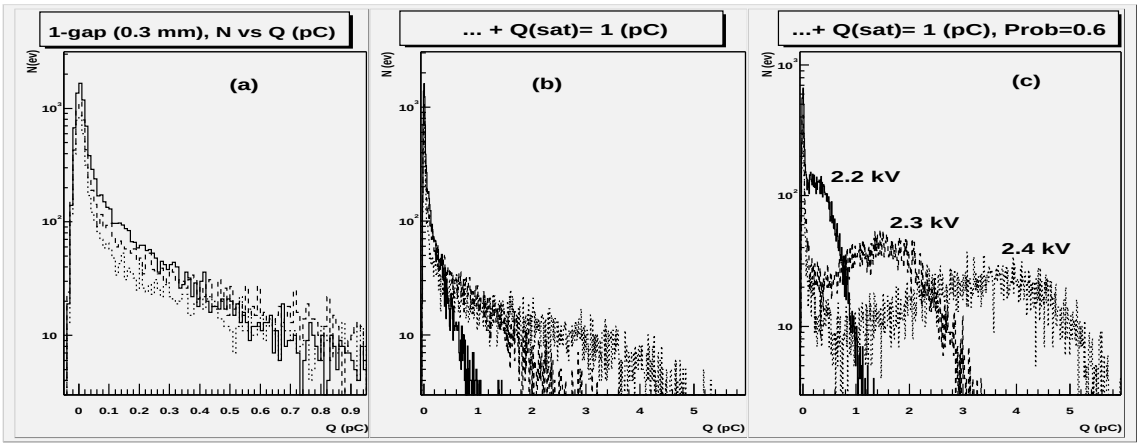

Figure 6. Charge distributions in 1-gap 0.3 mm for 3 different high voltage tension: 2.2, 2.3, 2.4 kV in the gas-gap. a) general simulation (no parameters used); b) $Q_{saturation}$= 1 pC; c) $Q_{saturation}$= 1 pC and Prob= 0.6.

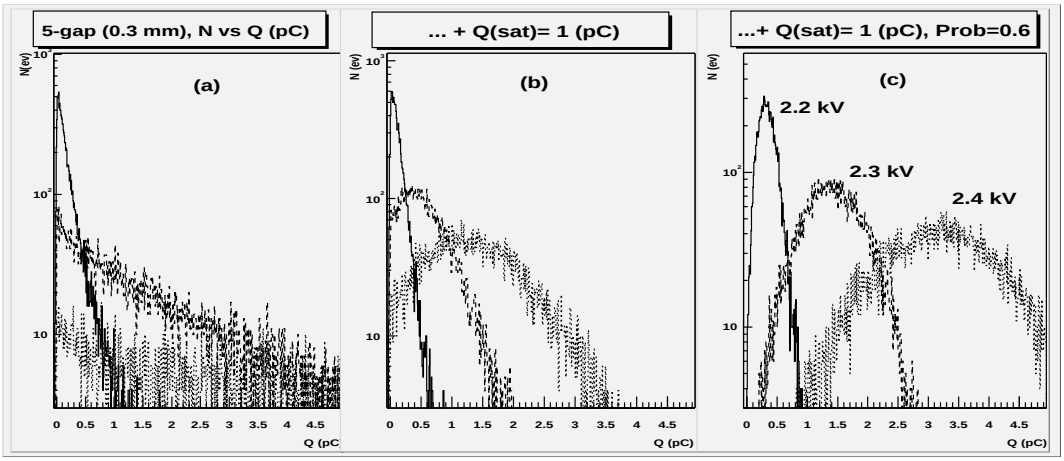

Figure 7. Charge distributions in 5-gaps (0.3 mm) for 3 different high voltage tension: 2.2, 2.3, 2.4 kV in the gas-gap. a) general simulation (no parameters used); b) $Q_{saturation}$= 1 pC; c) $Q_{saturation}$= 1 pC and Prob= 0.6.

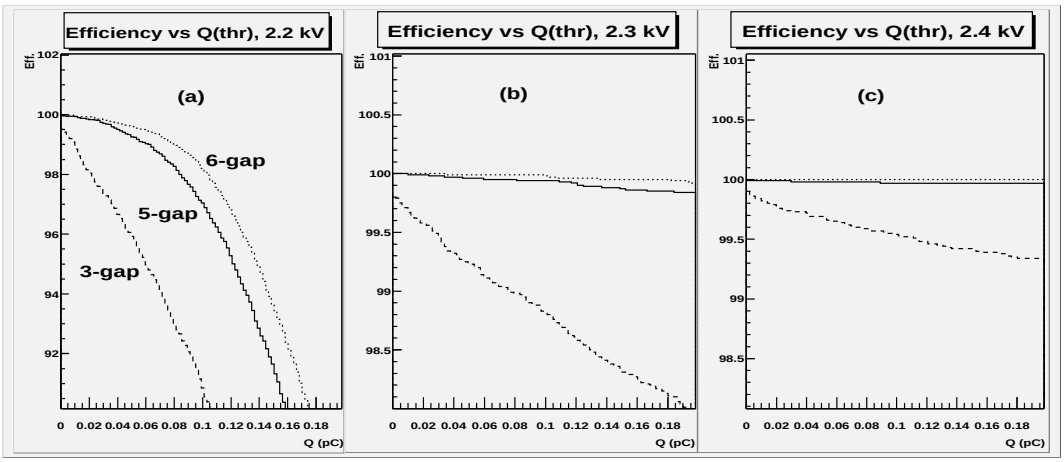

Figure 8. The efficiency of particle detection versus Q_{thres} for 3-,5-,6-gaps detectors for the cases of 3 different electric field tensions: a) 2.2 kV in the gap, b) 2.3 kV, c) 2.4 kV. Q_{sat}= 1 pC, Prob=0.6.

For the comparision, in Fig.7 the distributions obtained at the same conditions are presented for 5 gaps RPC prototype.

In Fig.8 one can see the efficiency of particle detection versus Q_{thres} for 3-,5-,6-gaps detectors for the cases of 3 different electric field tensions. The results are obtained for the presence of the saturation effect (Q_{sat}= 1 pC) and at the presence of an additional electron cluster with Prob=0.6.

In Fig. 9 the rising time of a signal is presented depending on the electric field tension in a gas-gap for the 5-gap prototype. Events at small values of "t" correspond to the cases of small amplitudes and the influence of a noise.

The dependence of the time of the signal starting versus the signal amplitude for the above 3 cases is presented in Fig. 10.

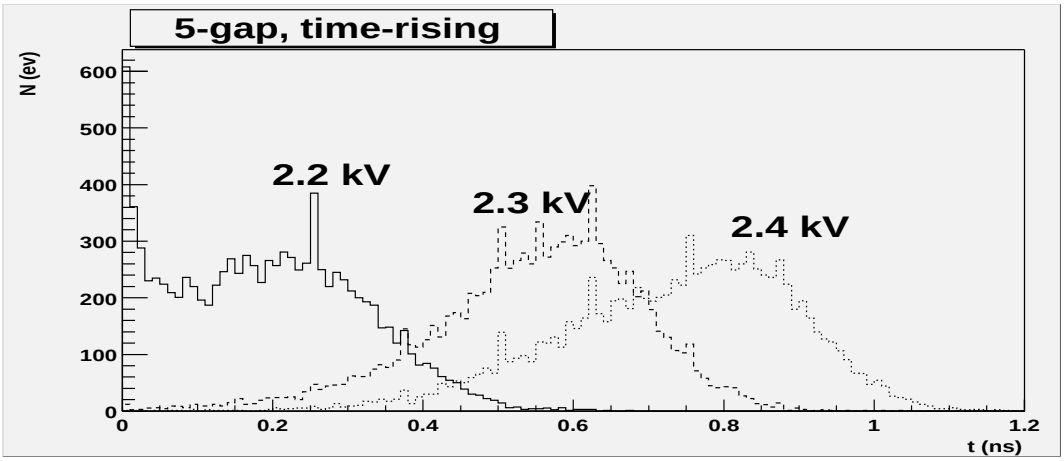

Figure 9. 5-gap, distribution of the rising time for 3 electric field tension: 2.2, 2.3, 2.4 kV in the gas-gap. $Q_{saturation}$= 1 pC and Prob= 0.6; gap= 0.3 mm.

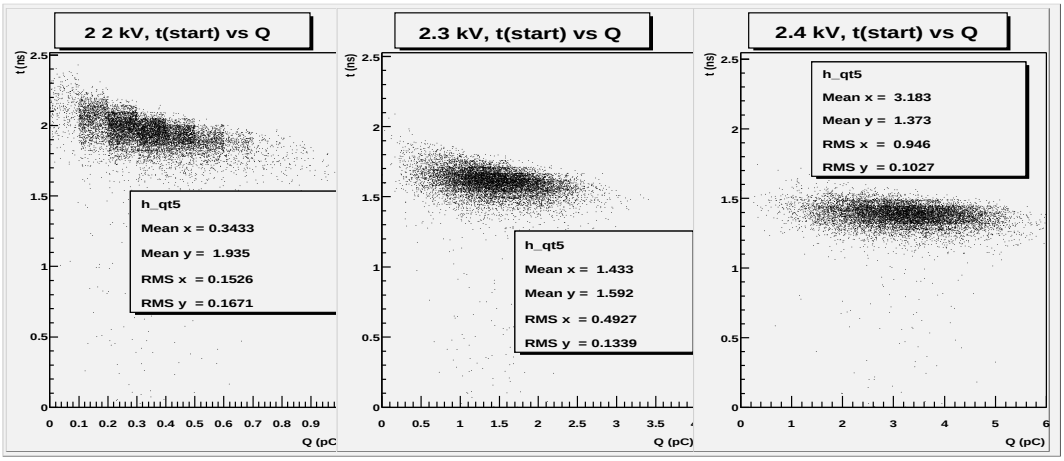

Figure 10. 5-gap, time of the signal registration vs the signal amplitude for 3 electric field tension: 2.2, 2.3, 2.4 kV in the gas-gap. $Q_{saturation}$= 1 pC and Prob= 0.6; gap = 0.3 mm.

Conclusions

It follows from the presented results that the better time resolution can be obtained for the less the gas-gap width. But this conclusion is obtained with the same value of the electronic noise level used. It is evident that for small values of the total collected charge (small gaps) one have to use another amplifiers with different values of the noise level. Therefore the real gas gap width can be chosen only in practic.

Another possibility to improve the time resolution is to rise the high voltage with the aim to use the high electron speed in a gap. At the same time in some investigations [22] it was observed that at sufficiently high electric field one has 2 types of the streamer discharges. They take place with the time delays about few nsec. That is why this possibility of the time resolution improvement is restricted.

According to the experimental data obtained for prototypes with approximately the same gas mixture and materials used one can suppose that for the analized prototype one has the following parameters for simulation: 1) the value of the saturation charge equals 1 pC; 2) the probability value of the additional electron cluster near the cathod surface equals 0.6. To take into account the possible noise effects the avalanche charge fluctuation is taken as in the case of general simulation (the standart Polya distribution).

The time-distributions for the fit are presented in Fig. 11, where errors are dispersion values of the corresponding time-distributions in each charge-bin in Fig. 10. These distributions are fitted by polynomial ("walk" correction). The 'corrected' time distributions (D(t)= t - "pol3") are presented in Fig.12, where "pol3" is a polynomial of the order 3.

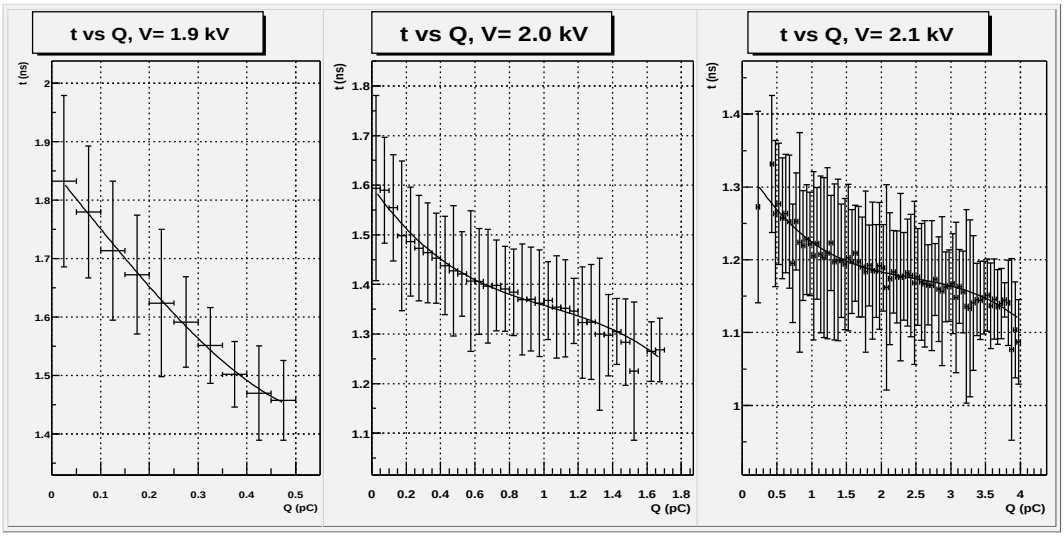

Figure 11. 5-gap, gap= 0.25 mm, average time-start dependence on the signal amplitude for 3 different electric field values: 1.9, 2.0, 3.0 kV in the gas-gap. Solid lines - fit-results by function "pol3".

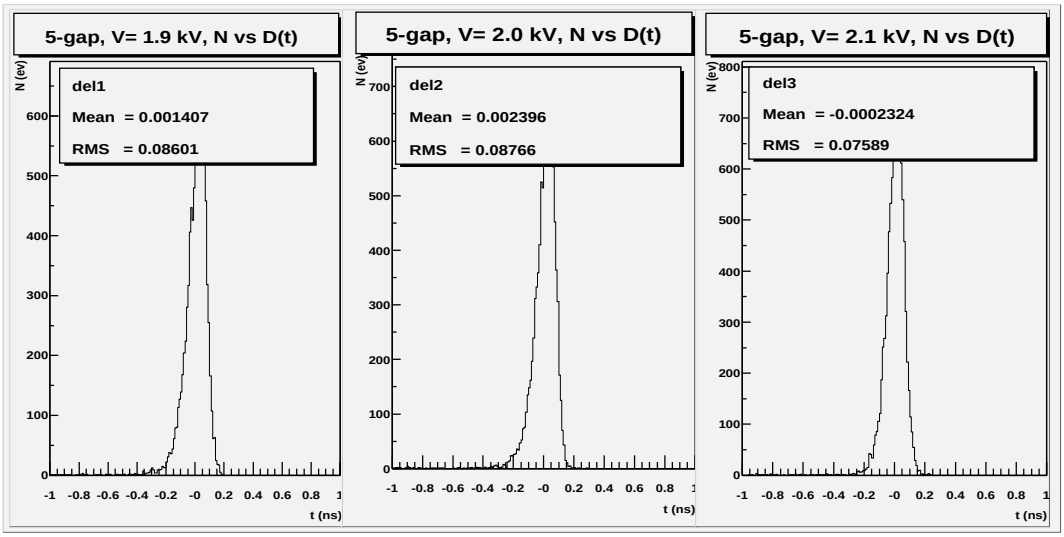

Figure 12. 5-gap, gap= 0.25 mm, time-"walk" corrected distributions for 3 electric field values: 1.9, 2.0, 2.1 kV in the gas-gap. $Q_{saturation}$= 1 pC and Prob= 0.6.

In Table 1 one can find the time-resolution values of the RPC prototype with the gas-gap width of 0.3 mm and for 3 electric field values in a gap: 2.2, 2.3, 2.4 kV. The results are presented for 5-gap and 6-gap prototypes with the gas mixture: 95% $C_2H_2F_4$ 5% *isobutane*. There were used the following simulation conditions: threshold = 0.05 pC, noise level = threshold/4, Q_{sat}= 1 pC, Prob= 0.6. The simulation results for gap= 0.25 mm and gap= 0.2 mm are presented in Tables 2 and 3. High voltage values in a gap are chosen in such way that the average collected charges are of the same order for all 3 cases of the gap values. In Table 2 there are shown also results for the case when the probability to have an additional electron cluster with "x=0" equals Prob= 0.3. These data are obtained with the total voltage in the range of 16-18 kV applied to the 5-gap prototype.

Table 1. The time resolution in "ns" (the dispertion of the time-starting distribution) for 5-gap and 6-gap RPC prototypes for the case of 3 electric field values in the gas-gap: 2.2, 2.3, 2.4 kV. Simulation parameters: threshold = 0.05 pC, noise= 0.0125 pC, Q_{sat}= 1 pC, Prob= 0.6. Gap= 0.3 mm.

N-Gap	E= 2.2 kV	E= 2.3 kV	E= 2.4 kV
5-gap	0.103	0.090	0.083
6-gap	0.099	0.087	0.080

Table 2. The time resolution in "ns" (the dispertion of the time-starting distribution) for 5-gap and 6-gap RPC prototypes for the case of 3 electric field values in the gas-gap: 1.9, 2.0, 2.1 kV. Simulation parameters: threshold = 0.05 pC, noise= 0.0125 pC, Q_{sat}= 1 pC, Prob= 0.6 (0.3). Gap= 0.25 mm.

N-Gap	E= 1.9 kV	E= 2.0 kV	E= 2.1 kV
5-gap	0.086 (0.100)	0.087 (0.092)	0.076 (0.079)
6-gap	0.085 (0.096)	0.084 (0.088)	0.074 (0.075)

Table 3. The time resolution in "ns" (the dispertion of the time-starting distribution) for 5-gap and 6-gap RPC prototypes for the case of 3 electric field values in the gas-gap: 1.65, 1.75, 1.85 kV. Simulation parameters: threshold = 0.05 pC, noise= 0.0125 pC, Q_{sat}= 1 pC, Prob= 0.6. Gap= 0.2 mm.

N-Gap	E= 1.65 kV	E= 1.75 kV	E= 1.85 kV
5-gap	0.073	0.073	0.057
6-gap	0.073	0.071	0.055

It is necceassary to mention that all figures in the Tables are "RMS" values of the corresponding distributions. This was done with the aim to show the electronic noise influence. When one takes into account the results of an approximation the time resolution achives the values of 50 ps with the gap of 0.25 mm.

For 5-gap and 6-gap prototypes results are very close to each other. 6-gap prototype is important as more efficient detector only for weak signals values but in our case we are going to "work" at the high electric field values and the 5-gap efficiency will be of the same order as it is in the case of the 6-gap prototype.

All presented results are obtained with fixed parameter values. At the same time it is known that parameters values depend on the electric field value (Q_{sat}, quantum efficiency to emit an electrons from the cathode-surface, ...). That is why the time-resolution dependence depicted in the Tables on the electric field must be stronger. These rusults one can consider as the first approximation.

The time-resolution of the TOF system at PHENIX amounts to about 110 ps, where 50 ps "comes" from BBC time-jittering of the "t0" parameter. Therefore for the RPC prototype to be as a TOF detector with 50 ps time resolution the final time resolution will come to approximately 80 ps.

Postscript

On finishing this article the new CERN-preprint was observed [23] devoted to the same topic. Authors of the preprint used another aproach to RPC simulation. The main difference in their simulation way is that they do not use the Prob-parameter (the probability to create additional electron cluster near a cathode). The experimental charge distributions are fitted owing to the unusual large η value. This Townsend coefficent value was calculated with their private verson of the MAGBOLTZ program: Imonte.

They ignore the possibility of an electron emission from glass plate surface. To our opinion this approach contradicts to the experimental data cited in the article.

References

[1] R.Santonico, NIM A456 (2000) 1.

[2] P.Fonte et al., NIM A477 (2002) 17, Prep. LIP/00-04 (2000);
P.Fonte et al., prep. CERN-EP/99-115 (1999).

[3] M.Abbrescia et al., NIM A431 (1999) 413.

[4] M.Abbrescia et al., NIM A398 (1997) 173;
M.Abbrescia et al., NIM A409 (1998) 1.

[5] P.Camarri et al., ATL-MUON-98-226 (1998).

[6] M.Abbrescia et al., Nucl.Phys. B(Proc.Suppl.) 78 (1999) 459.

[7] M.Abbrescia et al., NIM A414 (1998) 135.

[8] P.Fonte, NIM A456 (2000) 6.

[9] S.F.Biagi, NIM A283 (1989) 716;
S.F.Biagi, NIM A421 (1999) 234.

[10] R.Veenhof, CERN Program Library, 1998.

[11] I.Kitayama et al., NIM A424 (1999) 474.

[12] H.Fischle et al., NIM A301 (1991) 202.

[13] W.Blum, L.Roland, 1994, "Particle detection with drift chambers".

[14] J.T.Bromley, Thesis, the university of Manchester, 1994.

[15] V.Koreshev et al., NIM A456 (2000) 46;
V.Ammosov et al., IHEP Preprint 99-53, Protvino, 1999.

[16] A.Akindinov et al., NIM A456 (2000) 16.

[17] M.Abbrescie et al., NIM A392 (1997) 155.

[18] S.Ganter et al., NIM A414 (1998) 182.

[19] H.Raether, London, 1964, "Electron avalanches and breakdown in gases".

[20] V.Ammosov et al., IHEP Preprint 97-83, Protvino, 1997.

[21] V.Ammosov et al., IHEP Preprint 2002-10, Protvino, 2002, hep-ex/0204022.

[22] A.Semak et al., NIM A456 (2000) 50;
V.Ammosov et al., IHEP Preprint 2002-11, Protvino, 2002, hep-ex/0204026.

[23] V.Riegert et al., CERN-EP/2002-046, 2002.

Received October 29, 2002

Препринт отпечатан с оригинала-макета, подготовленного авторами.

В.В. Бабинцев, В.А. Бумажнов, Ю.В. Гилицкий, А.Г. Денисов
Моделирование высокоомной плоско-параллельной газовой камеры (RPC).

Оригинал-макет подготовлен с помощью системы **LaTeX.**

Подписано к печати 30.10.2002. Формат 60 × 84/8.
Офсетная печать. Печ.л. 2. Уч.-изд.л. 1.6. Тираж 60. Заказ 167.
Индекс 3649.

ГНЦ РФ Институт физики высоких энергий
142284, Протвино Московской обл.

Индекс 3649

П Р Е П Р И Н Т 2002–37, И Ф В Э, 2002